Discovery of a Highly Active Ligand of Human Pregnane X Receptor: A Case Study from Pharmacophore Modeling and Virtual Screening to "In Vivo" Biological Activity[S]

Géraldine Lemaire, Cindy Benod, Virginie Nahoum, Arnaud Pillon, Anne-Marie Boussioux, Jean-François Guichou, Guy Subra, Jean-Marc Pascussi, William Bourguet, Alain Chavanieu, and Patrick Balaguer

Institut National de la Santé et de la Recherche Médicale (INSERM) U824 (G.L., A.P., A.-M.B., P.B.) and INSERM, U632 (J.-M.P.), Montpellier, Université Montpellier 1, Montpellier, France; INSERM, U554, Montpellier, Université Montpellier 1 and 2, Centre National de la Recherche Scientifique, Unité Mixte de Recherche 5048, Centre de Biochimie Structurale, Montpellier, F-34090, France. (C.B., V.N., J.-F.G., G.S., W.B., A.C.)

Received December 22, 2006; accepted June 15, 2007

ABSTRACT

The human pregnane X receptor (hPXR) is a nuclear receptor that regulates the expression of phase I and II drug-metabolizing enzymes as well as that of drug transporters. In addition, this receptor plays a critical role in cholesterol homeostasis and in protecting tissues from potentially toxic endobiotics. hPXR is activated by a broad spectrum of low-affinity compounds including xenobiotics and endobiotics such as bile acids and their precursors. Crystallographic studies revealed a ligand binding domain (LBD) with a large and conformable binding pocket that is likely to contribute to the ability of hPXR to respond to compounds of varying size and shape. Here, we describe an in silico method that allowed the identification of nine novel hPXR agonists. We further characterize the compound 1-(2-chlorophenyl)-N-[1-(1-phenylethyl)-1H-benzimidazol-5-yl]methanesulfonamide (C2BA-4), a methanesulfonamide that activates PXR specifically and more potently than does the reference compound 4-[2,2-bis(diethoxyphosphoryl)ethenyl]-2,6-ditert-butyl-phenol (SR12813) in our stable cell line expressing a Gal4-PXR and a GAL4 driven luciferase reporter gene. Furthermore treatment of primary human hepatocytes with C2BA-4 results in a marked induction of the mRNA expression of hPXR target genes, such as cytochromes P450 3A4 and 2B6. Finally, C2BA-4 is also able to induce hPXR-mediated in vivo luciferase expression in HGPXR stable bioluminescent cells implanted in mice. The study suggests new directions for the rational design of selective hPXR agonists and antagonists.

The pregnane X receptor (PXR; NR1I2; (Lehmann et al., 1998), also known as steroid and xenobiotic receptor (Blumberg et al., 1998) and pregnane-activated receptor (Bertilsson et al., 1998), a member of the nuclear receptor superfamily, is a ligand-dependent transcription factor that regulates the expression of multiple drug-metabolizing enzymes and trans-porters in the liver and the intestine (Kliewer et al., 2002). PXR interacts with a variety of DNA response elements (direct repeats DR-3, DR-4, and DR-5, and everted repeats 6 and 8) in the 5′-flanking regions of genes as a heterodimer with the 9-cis retinoic acid X receptor (Blumberg et al., 1998; Xie et al., 2000; Kast et al., 2002). Upon ligand binding, the DNA-bound activated PXR/retinoid X receptor heterodimer recruits nuclear receptor coactivators thereby initiating the transcription of target genes (Kliewer et al., 2002; Orans et al., 2005). Johnson et al. (2006) demonstrated that the core-pressor SMRT binds and regulates the transcriptional activity of PXR.

PXR is a key regulator of phase I (cytochrome P450), phase II (conjugating), and phase III (ABC transporters) metabo-

ABBREVIATIONS: PXR, pregnane X receptor; DR, direct repeat; LBD, ligand-binding domain; h, human; SR12813, 4-[2,2-bis(diethoxyphosphoryl)ethenyl]-2,6-ditert-butyl-phenol; C2BA-4, 1-(2-chlorophenyl)-N-[1-(1-phenylethyl)-1H-benzimidazol-5-yl]methanesulfonamide; MD, molecular dynamic; PCR, polymerase chain reaction; RT-PCR, reverse transcription polymerase chain reaction; DMEM, Dulbecco's modified Eagle's medium; FCS, fetal calf serum; DMSO, dimethyl sulfoxide; PDB, Protein Data Bank; SMRT, silencing mediator for retinoic and thyroid hormone receptor.

lizing and detoxifying enzymes involved in endobiotic and xenobiotic clearance (Kliewer et al., 2002). Because a large number of prescription drugs activate the PXR pathway, PXR is thought to be involved in drug metabolism and efflux as well as in drug-drug interactions. Indeed, gene knockout studies confirmed a role for PXR in regulating the metabolism of endogenous steroids and xenobiotics (Staudinger et al., 2001). PXR is also involved in lipid homeostasis by activating genes that facilitate lipogenesis and by suppressing the β-oxidative pathways (Zhou et al., 2006). Even though PXR was identified as a xenobiotic sensor, some evidence suggests that PXR could be a potential therapeutic target for several human diseases. Recent studies indicate that PXR plays a role in bilirubin clearance and prevents hyperbilirubinemia and hepatorenal toxicity from cholesterol metabolites (Xie et al., 2003; Orans et al., 2005). Furthermore, it was recently shown that PXR ligands could be putative neuroprotectors in Niemann-Pick disease (Langmade et al., 2006).

Several agonists of hPXR have been described, including natural and synthetic steroids such as 5β-pregnane-3,20-dione and estradiol (Jones et al., 2000; Xue et al., 2007b), the cholesterol-lowering drugs lovastatin and SR12813 (Lehmann et al., 1998; Jones et al., 2000), the synthetic oxysterol ligand T0901317 (Xue et al, 2007a), the antibiotic rifampicin (Blumberg et al., 1998; Lehmann et al., 1998), and the active agent of St. John's wort, hyperforin (Wentworth et al., 2000). Crystal structures of the human PXR ligand-binding domain (hPXR LBD) revealed a typical three-layered α-helical sandwich, commonly found in nuclear receptors (Moras and Gronemeyer, 1998). However, PXR possesses a flexible and conformable ligand-binding pocket that adjusts its shape to accommodate ligands of distinct sizes and structures (Watkins et al., 2001, 2003). The large and conformable binding pocket probably contributes to its ability to respond to low-affinity compounds, including endobiotics (Chrencik et al., 2005; Xue et al., 2007b). Chrencik et al. (2005) reported the 2.8-Å resolution crystal structure of hPXR LBD in complex with the macrolide antibiotic rifampicin. They showed that rifampicin contacts 18 amino acid side chains in the PXR ligand-binding pocket through hydrogen bonds and hydrophobic interactions.

Because hPXR is a potential therapeutic target for several human pathologic conditions, new generation of hPXR modulators with improved selectivity and affinity for PXR might represent novel therapeutic tools. Furthermore, such ligands could serve as scaffold for the design of potent PXR antagonists (Synold et al., 2001; Tabb et al., 2004; Zhou et al., 2006).

In this report, we describe a structure-based and high-throughput virtual screening method that allowed discovering highly active PXR agonists. Based on the crystal structure of hPXR LBD in complex with rifampicin (Chrencik et al., 2005), we designed a pharmacophore and used this information to select the compound library, which was subsequently used for "in silico" screening. Using this approach, we were able to identify nine original hPXR agonists; one of them, C2BA-4, a methanesulfonamide, presents a higher activity than SR12813 on hPXR in biological assays.

Materials and Methods

Materials. Materials for cell culture, RNA extraction TRIzol reagent, SuperScript-II First-Strand Synthesis System for RT-PCR and Lipofectamine were from Invitrogen (Cergy-Pontoise, France). Luciferin and G418 were purchased from Promega (Charbonnières-les-Bains, France). SR12813 was purchased from Tebu-bio (Le Perray en Yvelines, France).

Virtual Screening. The structure-based design of new PXR agonists was performed using the crystal structure of hPXR LBD in complex with rifampicin [Protein Data Bank (PDB) code: 1SKX]. Hydrogen atoms were added to the protein structure by using the Insight II/Biopolymer-Discover3 modules (Accelrys Inc., San Diego, CA) at pH 7.0, and their positions were subjected to 1000 iterations of steepest descent minimization followed by 1000 steps of conjugate gradient minimization using the CFF force field. All nonhydrogen atoms of the protein as well as the ligand were held rigid during these minimizations. The X-ray structure of the complex was then heated and equilibrated at 298 K for 3 ps; amino acid side chains within a 5-Å distance from the ligand were unfixed while the rest of the protein was kept fixed. Then, at 298 K, a 5-ps molecular dynamic (MD) simulation with implicit water followed by an energy-minimization was repeated 50 times in the same condition of unfixed and fixed atoms, with total energy of interaction between hPXR and rifampicin monitored using the intermolecular command of the Discover3 module (Insight II; Accelrys). This energy evaluation was used to select the lowest energy-minimized LBD conformation among the last 10 MD-minimized structures. A heavy atom root-mean-square deviation value between selected and starting structures of the MD simulation was 0.39 Å, and both structures presented comparable LBD volumes. These two different target structures with the ligand removed were used for the virtual screening process. A two-dimensional database search was performed with the MDL.ISIS/Base software (http://www.mdli.com/) against the ChemBridge database (http://chembridge.com/chembridge/), and 496 molecules with specific pharmacophoric constraints were selected. These molecules retrieved in a multi-SDF file were converted to 3D structures (single conformation) with CORINA (Molecular Networks GmbH, Erlangen, Germany), then docked and evaluated by the Surflex v1.27 program (Jain, 2003). For virtual screening calculations, no water molecules were added during the protomol generation. For the two structures used, the poses of molecules with a score higher than 6, were visualized and analyzed.

Plasmids. The pPM-LBDhPXR expression plasmid was described previously (Ourlin et al., 2003). The yeast Gal4 DNA binding domain fused to the LBD of hPXR (107–434 amino acids) was generated from the pPM-LBD using PCR primers that introduced BamHI sites and subcloned into pSG5-puro (gift from Hinrich Gronemeyer, INSERM U184, Strasbourg, France).

The pET15b-hPXR expression plasmid was generated by PCR amplification of cDNA-encoding amino acids 107 to 434 of hPXR using oligonucleotides 5′-CGCGCGCATATGAAGGAGATGAT-CATG-3′ and 5′-GCGCGCGGATCCTCAGCTACCTGTGATGCCG-3′. All plasmids were fully sequenced.

Generation of Stable Reporter Cell Lines. HG$_5$LN and HG-PXR cells were described previously (Seimandi et al., 2005; Lemaire et al., 2006). In brief, HG$_5$LN cells were obtained by integration of a GAL4-responsive gene (GAL4RE$_5$-bGlob-Luc-SV-Neo) in HeLa cells (Seimandi et al., 2005). The HGPXR cell line was obtained by transfecting HG$_5$LN cells with a plasmid [pSG5-GAL4(DBD)-hPXR(LBD)-puro], which enables the expression of the DNA binding domain of the yeast activator GAL4 (Met1–Ser147) fused to the ligand binding domain of hPXR (Met107–Ser434) and confers resistance to puromycin. For the strain culture, cells were grown in Dulbecco's modified Eagle's medium (DMEM) containing phenol red and 1 g/l glucose, supplemented with 5% fetal calf serum (FCS) in a 5% CO2 humidified atmosphere at 37°C. HG$_5$LN cell medium was supplemented with 1 mg/ml G418 (Geneticin) and HGPXR cell medium with 1 mg/ml G418 and 0.5 μg/ml puromycin. For tests, cells were grown in DMEM without phenol red, supplemented with 3% dextran-coated charcoal-treated FCS.

Living Cell Luciferase Assay. Cells were seeded at a density of 5×10^4 cells per well in 96-well opaque white tissue culture plates and grown in 200 μl of DCC-FCS. Tested compounds were added 24 h later at concentrations between 10 nM and 10 μM, and cells were incubated for 16 h with compounds. At the end of incubation, compound-containing medium was removed and replaced by culture medium containing 0.3 mM luciferin. Luciferase activity was measured in a MicroBeta luminometer (PerkinElmer Life and Analytical Sciences–Wallac Oy, Turku, Finland) and luminescence was measured in intact cells for 2 s per well.

In Vivo Bioluminescent Imaging of HGPXR-Implanted Cells. The implantation technique of luminescent reporter cells was described earlier (Pillon et al., 2005; Lemaire et al., 2006). In brief, female athymic nude mice, approximately 50 days old and weighing 18 to 20 g, were obtained from Harlan France (Gannat, France) and acclimatized for a week before the experiment started. Mice were housed in self-contained filter-top plastic cages (four mice per cage) maintained under the following standard conditions: 22°C ± 2°C, 45% ± 10% relative humidity, 12-h light/dark cycle each day. Mice were given a standard diet (UAR, Epinay-sur-Orge, France) and water ad libitum.

Approximately 8×10^5 cells, prepared in serum-free DMEM, were subcutaneously grafted onto the mouse right dorsal flank (HGPXR cells) and left dorsal flank (HG$_5$LN cells, as an internal control); a week later, tumor size was considered sufficient for performing the in vivo experiments.

The PXR activities of different compounds were measured as follows. Mice were i.p. injected with 100 μl of C2BA-4, rifampicin, or SR12813 dissolved in DMSO at 25, 15, or 5 mg/kg of b.wt. Mice were imaged before injection and 8 h after injection. For bioluminescence imaging procedure, mice were first sedated using the isoflurane gas anesthesia system from T.E.M. (Bordeaux, France), with 4% isoflurane in air in an anesthesia induction box and then with 1.5% isoflurane in air/O$_2$ (80/20) continuously delivered via a nose cone system in the dark box of the NightOWL LB 983 NC100 CCD camera (Berthold Technologies, Bad Wildbad, Germany). Luciferase activity was then measured after the mice had been i.p. injected with luciferin saline solution, 125 mg/kg of b.wt., which gave rise to a luminescent signal that was maximal 10 min later and remained stable for 20 min. The photons emitted from luciferase were integrated for 2 min, and the pseudocolor luminescent image was generated using WinLight software (Berthold Technologies). A grayscale body-surface reference image was also collected. The overlay of the body image and the luminescence representation allowed the localization of the xenografts. The luminescent signal intensities from the regions of interest were obtained and the data were expressed as photon flux (photons per second). Background photon flux was defined from a region of interest of the same size placed in a nonluminescent area near the animal, and then subtracted from the measured luminescent signal intensity.

Mean values ± S.D. were calculated from at least four independent experiments. Statistical analysis of the results was carried out using one-way analysis of variance (ANOVA) with Tukey's post hoc test to evaluate the effect of SR12813 or C2BA-4. Six mice were necessary to accomplish the present work. All experiments were performed in compliance with the French guidelines for experimental animal studies (agreement no. B-34-172-27).

Limited Proteolytic Digestion. LBD of hPXR in pET-15b expression plasmid (1 μg) was generated by coupled transcription/translation in rabbit reticulocyte lysate using the TNT system according to the manufacturer's instructions (Promega, Madison WI). [^{35}S]Methionine was included in the transcription/translation mix to generate [^{35}S]PXR. In brief, after a 30-min incubation with ligand at room temperature, hPXR protein was digested at 25°C with 250 μg/ml trypsin for 10 min. Proteolysis was terminated by adding SDS sample buffer and boiling for 5 min.

The proteolytic fragments were separated on a 10% SDS-polyacrylamide gel. Gels were dried, and radiolabeled digestion products were visualized by autoradiography using a bioimaging analyzer (FUJIX BAS 1000; Fuji Medical Systems, Tokyo, Japan). Autoradiograms were evaluated using image analysis software. Experiments were performed three times. To measure the relative levels of the bands protected by a test compound on a gel, the intensity of the band of PXR-LBD treated with ethanol, around 30 kDa, was taken as 1.

Liver Samples, Hepatocyte Cultures, and Treatment. Hepatocytes were prepared from lobectomy segments resected from adult patients for medical purposes unrelated to our research program. The use of these human hepatic specimens for scientific purposes has been approved by the French National Ethics Committee.

Human hepatocytes were prepared and cultured as described previously (Pascussi et al., 2000). Cells were plated into collagen-coated P12 dishes at 0.17×10^{-6} cells/cm^2 in a hormonally and chemically defined medium consisting of a mixture of Williams' E and Ham's F-12 [1:1 (v/v)] media. Treatment with 10^{-6} M and 10^{-5} M effector solutions or solvent (0.1% DMSO) started 48 h after plating and lasted 24 h.

Total RNA Purification and CYP3A4 Quantitative PCR. Total RNA was isolated with TRIzol reagent. cDNA was synthesized from 1 μg of total RNA using the SuperScript II First-Strand Synthesis System for RT-PCR at 42°C for 60 min in the presence of random hexamers (Invitrogen), and then 10-fold diluted in water. Two microliters were used in duplicate for quantitative PCR amplification of CYP2B6, CYP3A4, and β-actin, as internal control, using the Light Cycler apparatus (Roche Diagnostic Corporation, Meylan, France). The following program was used: denaturation step at 95°C for 10 min, 45 cycles of PCR (denaturation at 95°C for 10 s, annealing at 65°C for 8 s, elongation at 65°C for 15 s). Primers were as follows: β-actin: forward, 5′-tgggcatggtgcagaaggat; reverse, 5′-tccatcacgatgccagtggt; CYP3A4: forward, 5′-cacaaaccggaggccttttg; reverse, 5′-atccatgctgtagggccccaa; CYP2B6: forward, 5′-ggccatacgggaggcccttg; reverse, 5′-agggccccttggatttccg. The curves of amplification were read with Light Cycler Software (Roche) using the comparative cycle threshold method. Relative quantifications of the target mRNAs were calculated after normalization of cycle thresholds with respect to the β-actin levels. Values are expressed as -fold induction compared with untreated cells (0.1% DMSO) ± S.D. For each donor, statistical analysis of the results was carried out using a two-sample, two-tailed Student's t test to evaluate the effect of rifampicin, SR12813, or C2BA-4 treatments on the control. Results were considered statistically significant at $p < 0.05$.

Data Analysis and Statistics. In the transactivation assay, each compound was tested at various concentrations in at least three separate experiments in triplicate wells and data are presented as the mean ± S.D. Individual agonist dose-response curves were fitted using the sigmoidal dose-response function of Prism software (version 4.0; GraphPad Software, San Diego, CA). The EC$_{50}$ for luciferase activity was calculated via nonlinear regression. This equation was used to fit the data in the graphic software. Transactivation data are presented as EC$_{50}$ values for each compound tested.

One-way analysis of variance was used to demonstrate statistical difference between the activity percentage of control and tested compounds with the help of GraphPad Prism. Calculation of statistical significance (P values < 0.05) between treated and controlled groups were performed using Tukey's post hoc test.
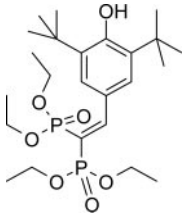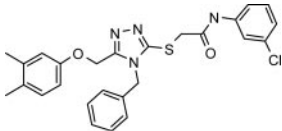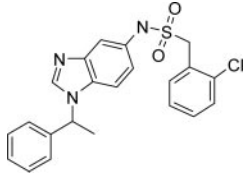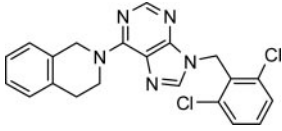
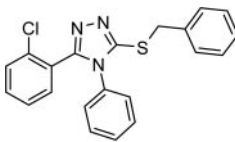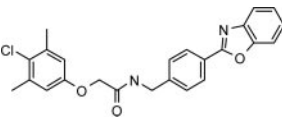## Results
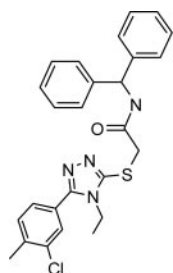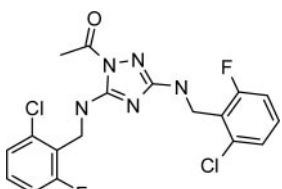
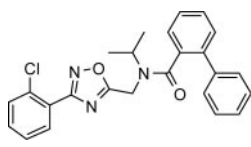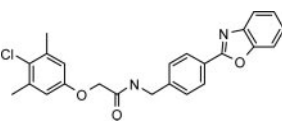**Structure-Based Design and Virtual Screening.** To rationalize the identification of original and highly active hPXR ligands, a structure-based approach was used. Crystal structures of the ligand-binding pocket of hPXR in complex with a variety of agonists (PDB codes 1SKX, 1NRL, and 1ILH) were analyzed to derive a pharmacophore model for potential ligands (Watkins et al., 2001, 2003; Chrencik et al.,

2005). As previously mentioned, the crystal structure of hPXR LBD in complex with rifampicin reveals a canonical fold consisting of a three layered-helical sandwich with, however, a unique five-stranded antiparallel β-sheet as well as a highly hydrophobic and flexible ligand binding pocket. Rifampicin, one of the largest PXR ligands identified thus far, interacts with 18 amino acid side chains of hPXR that are not all in contact with the smaller ligands. Indeed, comparison of all hPXR LBD structures reveals that only six residues are consistently involved in ligand binding (Supplementary Data I). Met243, Trp299, and Phe420 are involved in hydrophobic interactions, whereas Ser247, Gln285, and His407 form hydrogen bonds with the ligands (Orans et al., 2005). Based on these crucial interactions and in agreement with previously

reported pharmacophore models for PXR activators (Ekins and Erickson, 2002; Schuster and Langer, 2005), we built a two-dimensional pharmacophore made up of 2 to 4 hydrophobic phenyl groups and at least one hydrogen-bond acceptor that could form a hydrogen bond with polar residues. Then, on the basis of the chemical structure of known PXR ligands, we also selected compounds presenting 1) up to three hydrogen-bond donors, 2) a chlorine heteroatom, which is present in several PXR agonists, such as the pesticides chlordane or chlordecone (Lemaire et al., 2004; Kretschmer and Baldwin, 2005), and 3) two nitrogen atoms, allowing the formation of additional hydrogen bonds and the design of original molecules compared with reference ligands SR12813 and hyperforin. Finally, several molecular features were added to our

TABLE 1

Chemical structures and EC_{50} values of active PXR ligands obtained with HGPXR reporter cell lines. C2BA-4 is used as a racemic solution.

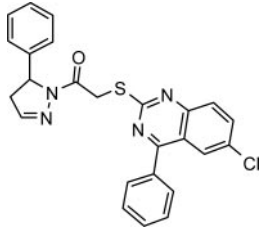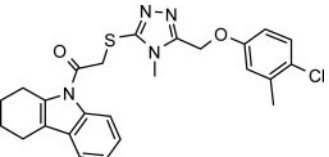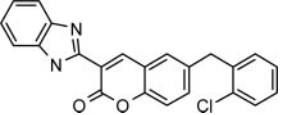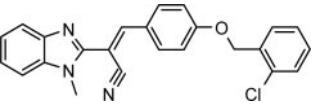| Name	Chemical Structure	EC_{50}	Name	Chemical Structure	EC_{50}
		nM			*nM*
SR12813		137 ± 45	C2BA-8		1308 ± 675
C2BA-4		49 ± 15	C2BA-10		163 ± 76
C2BA-5		2856 ± 1558	C2BA-13		191 ± 81
C2BA-6		1893 ± 790	C2BA-248		1893 ± 790
C2BA-7		108 ± 52	C2BA-251		108 ± 52

pharmacophoric constraints, such as a molecular mass up to 500 Da and a cLog P between 5 and 6 to favor membrane crossing. A subset of 496 molecules was so retrieved from the ChemBridge Database (February 2004) and docked using the Surflex program (Jain, 2003). The virtual screening was performed using the structure of the rifampicin-bound hPXR LBD described by Chrencik et al. (2005) with or without further MD optimization. After virtual screening (see *Materials and Methods*), docking poses of top-ranked molecules (score higher than 6) were visualized and analyzed for their associations with hydrophobic residues and their capabilities to form at least one hydrogen bond with Ser247, Gln285, or His407. At the final stage, six molecules were retrieved from the screening using the X-ray structure (C2BA-3, C2BA-7, C2BA-10, C2BA-11, C2BA-12, and C2BA-248), six from the MD structure (C2BA-4, C2BA-5, C2BA-6, C2BA-8, C2BA-13, and C2BA-251), and one (C2BA-9) obtained from both target structures. Table A in supplementary data provides ChemBridge IDs and docking scores for the 13 compounds (set I). Molecules that showed a promising docking mode were purchased for further biological evaluation.

C2BA-4 Was a Potent PXR Activator in HGPXR Cells. HGPXR cells obtained as described under *Materials and Methods* were designed to detect hPXR agonists, and the intermediary HG_5LN cell line allowed us to evaluate non–PXR-mediated luciferase gene expression. We first evaluated the 13 compounds identified by virtual screening for PXR activation using the HGPXR stable cell line. In a previous work (Lemaire et al., 2006), we studied the activities of the most potent known PXR ligands, rifampicin, hyperforin, and SR12813, on the HGPXR cell line. These ligands displayed full agonist activities with different EC_{50} values (720 ± 30, 110 ± 15, and 137 ± 45 nM, respectively). Because the

human and rabbit PXR activator SR12813 (Jones et al., 2000) had the highest activity, it was chosen as our reference molecule for this study, and the activation values obtained with all the tested compounds were expressed relative to the luciferase activity observed in the presence of 1 μM SR12813 and taken as 100. The baseline activity of the HGPXR cells was 21.3 ± 3.1%. The structures and EC_{50} values of original and reference ligands are displayed in Table 1 (active compounds) and Table 2 (inactive compounds) (see also set I; 9 of the 13 compounds showed agonistic activity (Fig. 1, A and B). They were categorized into three potency groups: weak (EC_{50} > 10 μM), moderate (1 μM < EC_{50} < 10 μM) (Fig. 1B), and strong (EC_{50} < 1 μM) (Fig. 1A).

Fig. 1. C2BA-4 is an efficient hPXR agonist. The activity of HGPXR cells was measured as a function of the concentration of potent inducers (SR12813, C2BA-4, C2BA-7, C2BA-10, and C2BA-13) (A) and SR12813 and moderate and weak inducers (C2BA-5, C2BA-6, C2BA-8, C2BA-248, and C2BA-251) (B). Activity was expressed as a percentage of 1 μM SR12813-induced activity. C, the activity of HG5LN control cells was measured at 0.3, 1, 3, and 10 μM C2BA-3, C2BA-7, C2BA-8, C2BA-10, C2BA-12, C2BA-13, and C2BA-248. Means ± S.D. were calculated from three independent experiments performed in triplicate.

TABLE 2
Chemical structures of inactive PXR ligands.

Compound	Chemical Structure
C2BA-3	
C2BA-9	
C2BA-11	
C2BA-12	

Four of them (C2BA-4, C2BA-7, C2BA-10, and C2BA-13) were found to be strong inducers of luciferase expression. EC_{50} values were 49, 108, 163, and 191 nM, respectively. C2BA-8, C2BA-6, and C2BA-5 were moderate inducers. Their EC_{50} values were 1306, 1893, and 2856 nM, respectively. Finally, C2BA-248 and C2BA-251 produced noticeable transactivation, but even at high concentration, luciferase expression did not reach 100%. The structures of inactive compounds (C2BA-3, C2BA-9, C2BA-11, and C2BA-12) are displayed in Table 2.

To evaluate the strength of our docking studies, we selected an additional set of 9 compounds (set II, see Table B in supplementary data) from the same subset of 496 molecules bearing the pharmacophoric constraints. In set II, we retrieved compounds that form fewer contacts with critical residues (cut-off distance 3 Å) but presenting a binding score higher than approximately 6. When tested for their activity, only one molecule was found to be a strong inducer ($EC_{50} <$ 1 μM) whereas four compounds had an EC_{50} ranking from 1 to 5 μM, and 4 molecules were inactive. Thus, this additional set of compounds led to less potent molecules compared with the 13 compounds of set I.

To assess the PXR-independent luciferase expression as well as the toxicity of the new compounds, all ligands were systematically tested for their ability to activate parent HG_5LN cells. Among molecules of set I, C2BA-12 and C2BA-3 showed luciferase activity in HG_5LN cells (Fig. 1C), demonstrating that the activity observed in HGPXR cells was non–PXR-specific. In addition, C2BA-7, C2BA-8, C2BA-10, C2BA-13, and C2BA-248 were toxic at 10 μM, and C2BA-7 and C2BA-13 were toxic at 5 μM (Fig. 1C). The toxicity of these compounds was also observed in HGPXR cells. At 1 μM, C2BA-7, C2BA-13, and C2BA-248 reached a plateau at 100% maximal HGPXR activity. At higher concentrations, a decrease in HGPXR luciferase expression was observed. For C2BA-8 and C2BA-248, the plateau was observed at 3 μM. Because C2BA-4 presented the lowest EC_{50} on HGPXR cells

as well as an absence of toxicity, this compound was selected for additional studies. No PXR-independent toxicity was observed for the nine compounds of set II (data not shown).

Limited Proteolytic Digestion. To determine whether C2BA-4 interacts directly with PXR and induces conformational changes, we analyzed the resistance of C2BA-4 hPXR to limited proteolysis (Fig. 2). hPXR LBD labeled with [35S]methionine was preincubated with ethanol (vehicle) or increasing concentrations (10.0, 3.0, 1.0, and 0.3 μM) of C2BA-4 or SR12813, before digestion with 250 μg/ml trypsin. The input lane represents undigested PXR (47 kDa). Incubation of the receptor with 250 μg/ml trypsin in the absence of ligand (ETOH) led to complete digestion of hPXR-LBD. In contrast, SR12813 produced a 30-kDa major protease-resistant fragment after partial protease digestion. The protease protection pattern induced by C2BA-4 was similar to that obtained with SR12813. C2BA-4 was slightly more potent at 0.3 μM, but a higher degree of protection was obtained with SR12813 at 10 μM (Fig. 2). These results indicate that the two ligands interact directly with hPXR LBD and induce similar conformational changes.

C2BA-4 Induces CYP3A4 and CYP2B6 Expression in Human Hepatocytes. The effect of C2BA-4 on PXR target gene expression was further evaluated in human hepatocytes. Cultured human hepatocytes from four different donors were treated with the control solvent (0.1% DMSO), rifampicin (5 or 10 μM), SR12813 (1 μM), or C2BA-4 (5 μM) for 24 h. Total mRNA was isolated, and quantitative RT-PCR was performed to detect the expression level of CYP3A4 and CYP2B6 mRNAs. As expected, rifampicin and SR12813 strongly and significantly increased CYP3A4 and CYP2B6 mRNA expressions in these cells (Table 3). More interestingly, C2BA-4 induced the expression of CYP3A4 (from 8- to 74-fold induction compared with untreated cells) and CYP2B6 (from 3- to 46-fold induction compared with untreated cells) mRNAs in all culture preparations tested. In addition, we observed that the increase of CYP3A4 and
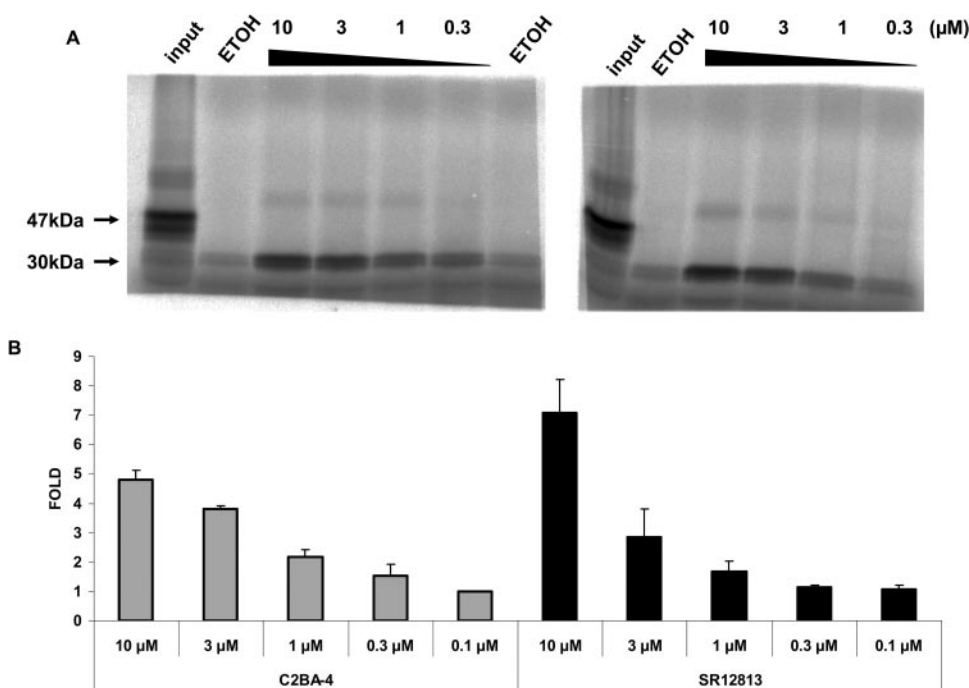

Fig. 2. Binding of C2BA-4 to PXR. PXR protein was synthesized and labeled with [35S]methionine in reticulocyte lysate and incubated with C2BA-4 and SR12813 or vehicle alone before trypsin digestion. The reaction was terminated by boiling in SDS-containing protein sample buffer. PXR proteolytic pattern was analyzed by SDS-PAGE and fixed/dried gel were visualized by filmless autoradiographic analysis. A, C2BA-4 and SR12813 treatments protect from trypsin digestion in dose-dependent manner. A trypsin resistant fragment (30 kDa) was generated in presence C2BA-4 and SR12813. Figure shown is representative of three experiments. B, autoradiograms were analyzed using image analysis software. To measure the relative levels of the 30-kDa band protected by C2BA-4 or SR12813 on an SDS-polyacrylamide gel, the intensity of the band of PXR-LBD treated with ethanol was taken as 1.

TABLE 3
Effect of C2BA-4 on the expression of PXR target genes in cultured human hepatocytes

Human hepatocytes from four different donors were treated for 24 h with solvent (0.1% DMSO), rifampicin (5 or 10 μM), SR12813 (1 μM), or C2BA-4 (5 μM). Twenty hours later, cells were harvested in TRIzol, total RNA was extracted, and cDNA was synthesized. CYP3A4 and CYP2B6 levels were measured via quantitative real-time PCR using the Light Cycler apparatus. As an internal control, the β-actin mRNA level was measured similarly to normalize data. Data are expressed as -fold induction compared with nontreated cells ± S.D. $P < 0.05$ unless noted otherwise.

	Donor 1 (FT259)		Donor 2 (FT261)		Donor 3 (FT267)		Donor 4 (FT268)	
	CYP3A4	CYP2B6	CYP3A4	CYP2B6	CYP3A4	CYP2B6	CYP3A4	CYP2B6
Rifampicin	49.92 ± 6.95	10.22 ± 1.43	35.79 ± 0.53	11.53 ± 0.4	19.82 ± 6.68	25.85 ± 9.35	15.12 ± 0.71	6.17 ± 0.8
SR12813	N.D.	N.D.	21.08 ± 2.48	23.39 ± 1.69	47.21 ± 15.79	26.71 ± 10.11	4.14 ± 1.71	2.70 ± 1.23*
C2BA-4	74.07 ± 8.71	46.06 ± 5.58	23.38 ± 0.45	31.26 ± 2.27	13.13 ± 3.3	8.68 ± 2.17	8.37 ± 1.38	3.65 ± 0.44

N.D., none determined.
* $P > 0.05$.

CYP2B6 by C2BA-4 was dose-dependent in FT259 (Fig. 3) and very close to that obtained with rifampicin. These results demonstrate that, in agreement with our in vitro studies, C2BA-4 is able to activate PXR in human hepatocytes, leading to an increase of transcription of its main target genes such as CYP3A4 and CYP2B6.

In Vivo Response of Xenografts to hPXR Ligands. To test C2BA-4 activity in the context of the whole organism, HGPXR cells were implanted in nude mice (Fig. 4), as described previously (Lemaire et al., 2006). Mice were subcutaneously grafted with HGPXR cells onto the right dorsal flank and with HG_5LN cells as an internal control onto the left dorsal flank, as described under *Materials and Methods*. The luminescent signal was detected before (Fig. 4, A and C) and 8 h after (Fig. 4, B and D) i.p. injection of 25 mg/kg SR12813 or C2BA-4 using a CCD camera. The specific responses in the HGPXR tumor were normalized by taking into account the basal response obtained in the HG_5LN tumor before calculation of the -fold induction. Detailed photon counting (photons per second) and induction factor calculation are reported in Fig. 4E. Although signal intensities could be different from one mouse to another because of a difference in tumor size, induction factors were reproducible. HG_5LN internal control was used to detect nonspecific activation of luciferase promoter and to detect any reproducibility problems as a result substrate i.p. injection that may cause variations in luciferin bioavailability and perturb signal intensity. Injection of 5, 15, and 25 mg/kg SR12813 or C2BA-4 caused a dose dependant increase in the induction factor (Fig. 4F). At 25 mg/kg, induction factor averages of SR12813 and C2BA-4 were 2.5 ± 1 and 2.2 ± 0.8, respectively.

Discussion

PXR has a central role in human detoxification biology, regulating the expression of a critical set of gene products involved in xenobiotic and endobiotic metabolism. Thus, agonists of hPXR enhancing the removal of endogenous and exogenous toxins are potential pharmacological tools and therapeutic agents. Recent studies suggest that treatment with PXR activators may delay the progressive degeneration of Niemann-Pick C1 disease (Langmade et al., 2006). Furthermore, such ligands could be used as scaffold for the design of compounds with antagonistic activity (Bourguet et al., 2000; Steinmetz et al., 2001; Shiau et al., 2002; Xue et al., 2007a). Development of PXR antagonists is desirable as a potential way to control the up-regulation of drug metabolism pathways during some therapeutic treatments.

Using a computational approach, the aim of our study was to identify original agonistic ligands. A structure-based approach to design ligands for hPXR requires a consideration of three characteristics of hPXR LBD: 1) a large size, 2) a high flexibility with dynamic accommodations, and 3) the hydrophobic nature of key residues implicated in the interaction with ligands. Indeed, by contrast with other nuclear receptors, hPXR contains a 60-amino acid insertion located in the binding site, which seems to account for the first two characteristics. Moreover, the absence of salient features of the LBD in terms of shape and electrostatic potential was reported as unfavorable for the efficiency of a virtual screening on hPXR (Schapira et al., 2003). These particular characteristics of PXR limit the effectiveness of a structure-based design approach. However, as mentioned by Orans et al.

(2005), six amino acid side chains were found to be involved in ligand binding in all the LBD structures of hPXR determined to date. Thus, from among the Surflex docking results

with a score higher than 6, we selected a set of 13 molecules interacting with these residues via a combination of hydrophobic contacts and hydrogen bonds. From these 13 com-
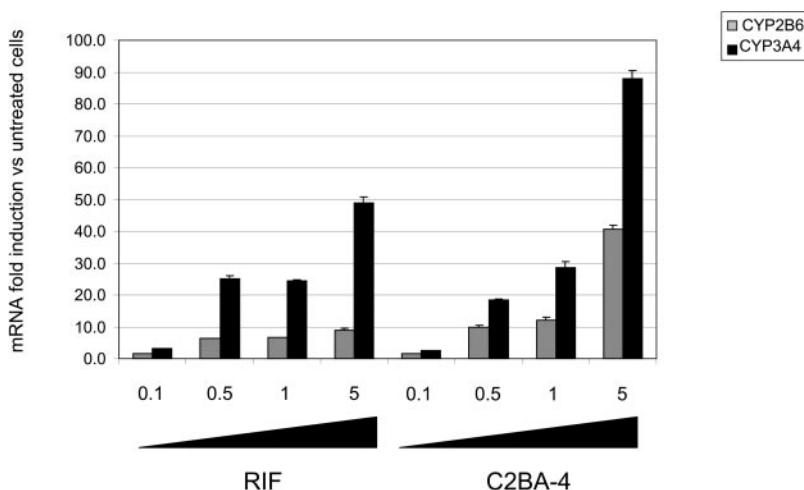

Fig. 3. Dose-dependent effect of C2BA-4 on CYP3A4 and CYP2B6 gene expression in cultured human hepatocytes. Human hepatocytes from FT259 were treated for 24 h with solvent (0.1% DMSO), rifampicin, and C2BA-4 at different concentrations ranging from 0.1 to 5 μM as indicated. Twenty hours later, cells were harvested in TRIzol, total RNA was extracted, and CYP3A4 and CYP2B6 levels were measured via quantitative real-time PCR using the Light Cycler apparatus. As an internal control, the β-actin mRNA level was measured similarly to normalize data. Data are represented as -fold induction compared with nontreated cells ± S.D.
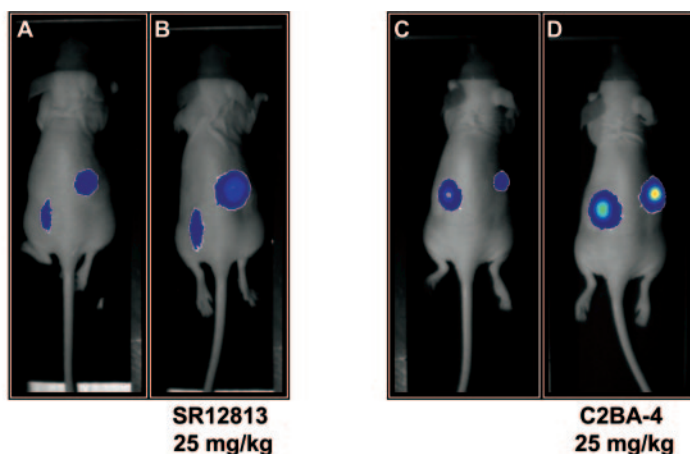
		Light emitted from xenograft			Induction factor
		HG5LN (photons/s)	HGPXR (photons/s)	Relative to HG5LN	
SR12813	0 h	9676	25583	2.64	2.7
	8 h	20506	143948	7.02	
C2BA-4	0 h	41360	12151	0.29	3.2
	8 h	137719	131018	0.95	

Fig. 4. Effect of C2BA-4 on in vivo induction of hPXR in nude mice. A–D, bioluminescent imaging of nude mouse xenografts: HG5LN (left flank) and HGPXR (right flank) xenograft were imaged before (A) and 8 h after (B) 25 mg/kg SR12813 i.p. injection or before (C) and 8 h after (D) 25 mg/kg C2BA-4 i.p. injection. E, photon counting and induction factors of HG5LN and HGPXR xenografts before and after stimulation by 25 mg/kg SR12813 or C2BA-4. Light intensities (photons per second) were calculated using WinLight software (Berthold Technologies) as described by Pillon et al. (2005). Specific signal was background subtracted and ratio of HGPXR specific values relative to HG5LN gives the induction factor for SR12813 or C2BA-4. F, SR12813, and C2BA-4 were i.p. injected in nude mice at the indicated concentrations (milligrams per kilogram) to establish in vivo dose response curves. Mean values ± were calculated from four independent experiments, and six mice were necessary to perform in vivo experiments.
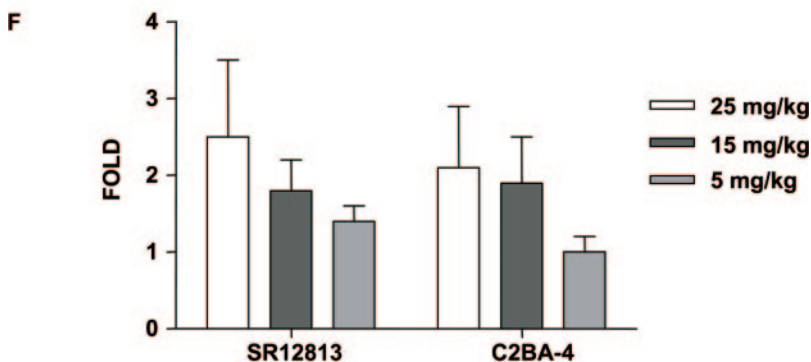
pounds, 9 were found to exhibit an agonistic activity (Table 1), 3 came from the virtual screening performed with the X-ray hPXR-rifampicin complex structure whereas 6 agonistic compounds were retrieved from docking on an MD-optimized complex conformation. The two LBD conformations led to the identification of highly active compounds with EC_{50} below 200 nM (Table A, set I, supplementary data).

Using an additional set of 9 compounds that presented a less favorable mode of binding as judged by proximity with the 6 critical residues, we also identified 5 additional ligands of hPXR but with less potent activity (Table B, set II, supplementary data). Taken together, these results clearly validate the pharmacophoric constraints employed and underline the potential of virtual screening in PXR agonist discovery. Furthermore, they suggest that the criterion of proximity with the 6 critical residues seems to be a good filter to identify highly active compounds even in the case of hPXR, which can adapt its LBD to many molecules.

One of the new hPXR ligands, C2BA-4 [1-(2-chlorophenyl)-*N*-[1-(1-phenylethyl)-1*H*-benzimidazol-5-yl]methanesulfonamide], was found to have no toxic effect and was able to activate hPXR with a better EC_{50} than SR12813 (Table 1), which led us to consider C2BA-4 as a potential hPXR ligand. Indeed, in a partial trypsin digestion assay, C2BA-4 effectively protected hPXR from trypsin digestion (Fig. 2), demonstrating a direct receptor-ligand interaction. C2BA-4 altered the protease sensitivity of hPXR and generated ligand-protection patterns similar to those observed for the SR12813-bound receptor. Moreover, our results show that C2BA-4 can alter the conformation of hPXR at a lower concentration than does SR12813 (Fig. 2), suggesting that C2BA-4 displays a higher affinity. To further characterize C2BA-4 as a potent PXR ligand, we studied its effect on CYP3A4 and CYP2B6 transcription (Xie et al., 2000) in primary culture of human hepatocytes. The current study shows that C2BA-4 induces an increase of CYP3A4 and CYP2B6 mRNA levels in human hepatocytes from 4 different donors and after 24 h of exposure with an efficacy comparable with that of rifampicin or SR12813. The response levels were different between donors because CYP3A4 and CYP2B6 are inducible enzymes and their induction varies markedly (up to 40-fold) across the population as a result of drug-mediated variation in cytochrome P450 transcription (Lamba et al., 2005).

Activation of hPXR and induction of drug-metabolizing enzymes in vitro may not imply that there is relevant induction of PXR-mediated gene in rodent or in human. To test whether C2BA-4 induces PXR activity in vivo, we implanted the HGPXR reporter cells in nude mice. This assay allowed an in vivo detection of C2BA-4 response; the advantage of our model is that we were able to measure human and not mouse PXR activation. Despite the better in vitro effectiveness of C2BA-4 compared with SR12813, our data obtained in primary human hepatocytes and in grafted nude mice show that C2BA-4 and SR12813 similarly activated hPXR. Differences in the bioavailability or metabolism of the two compounds might account for this apparent discrepancy.

Taken together, these results indicate that C2BA-4 represent a new potent agonist ligand of hPXR and could serve as novel lead for further chemical optimizations and pharmacological investigations. The putative most relevant mode of binding of this compound presented in Fig. 5, docked either

in X-ray and MD-derived structures, was found to be very close to that of the rifampicin (Chrencik et al., 2005; supplementary data 1). Indeed, the sulfonamide moiety of C2BA-4 could be hydrogen-bonded with Ser247 and His407 in the central part of the cavity as does rifampicin, which forms one hydrogen bond with Ser247, one with His407 and two with Gln285. The 1-phenylethyl moiety of C2BA-4 could interact with Trp 299 and the 2-chloro-benzyl group with Phe420 (Fig. 5). These two residues are systematically implicated in the agonist binding to hPXR. In addition, C2BA-4 seems to be at interacting distance with Val211 and Leu239, which participate in the binding of rifampicin, but not SR12813 or hyperforin (Chrencik et al., 2005). Then, it is interesting to note the proximity of the 2-chloro-benzyl group with residues forming helix 12 of the hPXR LBD, in particular Met425 (Fig. 5). In several nuclear receptors, helix 12 plays an important role, in that its position and its mobility, which vary according to the agonistic or antagonistic nature of the ligand, determine the interacting interface and the type of cofactor proteins that could bind to nuclear receptors. Thus, in several studies (Bourguet et al., 2000), it has been observed that bulky antagonistic ligands prevent helix 12 from adopting the active conformation of LBD.

This putative mode of binding of C2BA-4 will be useful for the rational design of analogs able to present additional contacts with the hPXR LBD. Indeed, the chemical structure of C2BA-4 opens the way to the synthesis of a large number of chemical analogs that could be investigated to develop agonistic compounds with higher activity. Moreover, cocrystallization studies of C2BA-4 in complex with hPXR are under progress to validate the mode of binding.

An article describing a new commercially available LXR and PXR ligand (T0901317) has been published (Xue et al., 2007a). Using transient PXR and LXR transfection, this new ligand showed EC_{50} values of 12.6 and 100 nM for PXR and LXR, respectively. It is noteworthy that T0901317 derivatives designated to obtain PXR antagonists were found to be potent agonists with an enhanced selectivity and affinity for PXR (EC_{50} of 3 nM and >10 μM for PXR and LXR, respectively). The promiscuity and the structural conformability of the PXR ligand binding pocket make antagonist design par-
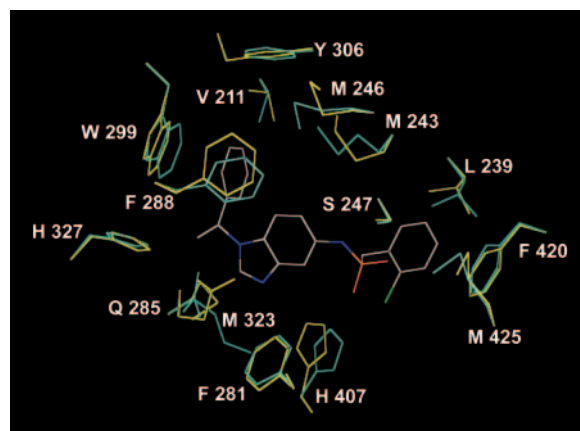

Fig. 5. Putative mode of binding for C2BA-4 in the ligand binding pocket of hPXR.C2BA-4 could form hydrogen bonds with at least Ser247 and His407 and hydrophobic contacts with Met243, Phe420, and Trp299. Hydrogens are not represented for clarity. The crystallographic structure of hPXR (PDB code 1SKX) is represented in yellow, and the MD structure of hPXR is in blue.

ticularly difficult. However, based on the putative mode of binding of C2BA-4, several C2BA-4 analogs with bulky substituent groups on the chlorophenyl moiety could be designed in an attempt to reverse the agonistic activity toward an original antagonistic action by preventing helix 12 from adopting an active conformation. If successful, the finding of hPXR antagonists could provide a unique tool to control drug metabolism and to reduce the activation of xenobiotic metabolism pathways during therapeutic treatment of disease. Finally, the virtual screening approach described in this report could represent a framework to develop relevant in silico tests to predict the ability of environmental compounds to bind PXR.

Conclusion

The current study represents a strategy for the identification of hPXR ligands by combining a structure-based design with a functional approach using both cell culture and whole animals. The original agonists described here, particularly the most active, will be further optimized chemically to design novel selective hPXR modulators with anticipated improved therapeutic indexes and great medical benefit.

References

Bertilsson G, Heidrich J, Svensson K, Asman M, Jendeberg L, Sydow-Backman M, Ohlsson R, Postlind H, Blomquist P, and Berkenstam A (1998) Identification of a human nuclear receptor defines a new signaling pathway for CYP3A induction. *Proc Natl Acad Sci U S A* **95:**12208–12213.

Blumberg B, Sabbagh W Jr, Juguilon H, Bolado J Jr, van Meter CM, Ong ES, and Evans RM (1998) SXR, a novel steroid and xenobiotic-sensing nuclear receptor. *Genes Dev* **12:**3195–3205.

Bourguet W, Germain P, and Gronemeyer H (2000) Nuclear receptor ligand-binding domains: three-dimensional structures, molecular interactions and pharmacological implications. *Trends Pharmacol Sci* **21:**381–388.

Chrencik JE, Orans J, Moore LB, Xue Y, Peng L, Collins JL, Wisely GB, Lambert MH, Kliewer SA, and Redinbo MR (2005) Structural disorder in the complex of human pregnane X receptor and the macrolide antibiotic rifampicin. *Mol Endocrinol* **19:**1125–1134.

Ekins S and Erickson JA (2002) A pharmacophore for human pregnane X receptor ligands. *Drug Metab Dispos* **30:**96–99.

Jain AN (2003) Surflex: fully automatic flexible molecular docking using a molecular similarity-based search engine. *J Med Chem* **46:**499–511.

Johnson DR, Li CW, Chen LY, Ghosh JC, Chen JD (2006) Regulation and binding of pregnane X receptor by nuclear receptor corepressor silencing mediator of retinoid and thyroid hormone receptors (SMRT). *Mol Pharmacol* **69:**99–108.

Jones SA, Moore LB, Shenk JL, Wisely GB, Hamilton GA, McKee DD, Tomkinson NC, LeCluyse EL, Lambert MH, Willson TM, Kliewer SA, and Moore JT (2000) The pregnane X receptor: a promiscuous xenobiotic receptor that has diverged during evolution. *Mol Endocrinol* **14:**27–39.

Kast HR, Goodwin B, Tarr PT, Jones SA, Anisfeld AM, Stoltz CM, Tontonoz P, Kliewer S, Willson TM, and Edwards PA (2002) Regulation of multidrug resistance-associated protein 2 (ABCC2) by the nuclear receptors pregnane X receptor, farnesoid X-activated receptor, and constitutive androstane receptor. *J Biol Chem* **277:**2908–2915.

Kliewer SA, Goodwin B, and Willson TM (2002) The nuclear pregnane X receptor: a key regulator of xenobiotic metabolism. *Endocr Rev* **23:**687–702.

Kretschmer XC and Baldwin WS (2005) CAR and PXR: xenosensors of endocrine disrupters? *Chem Biol Interact* **155:**111–128.

Lamba J, Lamba V, and Schuetz E (2005) Genetic variants of PXR (NR1I2) and CAR (NR1I3) and their implications in drug metabolism and pharmacogenetics. *Curr Drug Metab* **6:**369–383.

Langmade SJ, Gale SE, Frolov A, Mohri I, Suzuki K, Mellon SH, Walkley SU, Covey DF, Schaffer JE, and Ory DS (2006) Pregnane X receptor (PXR) activation: A mechanism for neuroprotection in a mouse model of Niemann-Pick C disease. *Proc Natl Acad Sci U S A* **103:**13807–13812.

Lehmann JM, McKee DD, Watson MA, Willson TM, Moore JT, and Kliewer SA (1998) The human orphan nuclear receptor PXR is activated by compounds that regulate CYP3A4 gene expression and cause drug interactions. *J Clin Invest* **102:**1016–1023.

Lemaire G, de Sousa G, and Rahmani R (2004) A PXR reporter gene assay in a stable cell culture system: CYP3A4 and CYP2B6 induction by pesticides. *Biochem Pharmacol* **68:**2347–2358.

Lemaire G, Mnif W, Pascussi JM, Pillon A, Rabenoelina F, Fenet H, Gomez E, Casellas C, Nicolas JC, Cavailles V, Duchesne MJ, and Balaguer P (2006) Identification of new human pregnane X receptor ligands among pesticides using a stable reporter cell system. *Toxicol Sci* **91:**501–509.

Moras D and Gronemeyer H (1998) The nuclear receptor ligand-binding domain: structure and function. *Curr Opin Cell Biol* **10:**384–391.

Orans J, Teotico DG, and Redinbo MR (2005) The nuclear xenobiotic receptor pregnane X receptor: recent insights and new challenges. *Mol Endocrinol* **19:**2891–2900.

Ourlin JC, Lasserre F, Pineau T, Fabre JM, Sa-Cunha A, Maurel P, Vilarem MJ, and Pascussi JM (2003) The small heterodimer partner interacts with the pregnane X receptor and represses its transcriptional activity. *Mol Endocrinol* **17:**1693–1703.

Pascussi JM, Gerbal-Chaloin S, Fabre JM, Maurel P, and Vilarem MJ (2000) Dexamethasone enhances constitutive androstane receptor expression in human hepatocytes: consequences on cytochrome P450 gene regulation. *Mol Pharmacol* **58:**1441–1450.

Pillon A, Servant N, Vignon F, Balaguer P, and Nicolas JC (2005) In vivo bioluminescence imaging to evaluate estrogenic activities of endocrine disrupters. *Anal Biochem* **340:**295–302.

Schapira M, Abagyan R, and Totrov M (2003) Nuclear hormone receptor targeted virtual screening. *J Med Chem* **46:**3045–3059.

Schuster D and Langer T (2005) The identification of ligand features essential for PXR activation by pharmacophore modeling. *J Chem Inf Model* **45:**431–439.

Seimandi M, Lemaire G, Pillon A, Perrin A, Carlavan I, Voegel JJ, Vignon F, Nicolas JC, and Balaguer P (2005) Differential responses of PPARalpha, PPARdelta, and PPARgamma reporter cell lines to selective PPAR synthetic ligands. *Anal Biochem* **344:**8–15.

Shiau AK, Barstad D, Radek JT, Meyers MJ, Nettles KW, Katzenellenbogen BS, Katzenellenbogen JA, Agard DA, and Greene GL (2002) Structural characterization of a subtype-selective ligand reveals a novel mode of estrogen receptor antagonism. *Nat Struct Biol* **9:**359–364.

Staudinger J, Liu Y, Madan A, Habeebu S, and Klaassen CD (2001) Coordinate regulation of xenobiotic and bile acid homeostasis by pregnane X receptor. *Drug Metab Dispos* **29:**1467–1472.

Steinmetz AC, Renaud JP, and Moras D (2001) Binding of ligands and activation of transcription by nuclear receptors. *Annu Rev Biophys Biomol Struct* **30:**329–359.

Synold TW, Dussault I, and Forman BM (2001) The orphan nuclear receptor SXR coordinately regulates drug metabolism and efflux. *Nat Med* **7:**584–590.

Tabb MM, Kholodovych V, Grun F, Zhou C, Welsh WJ, Blumberg B (2004) Highly chlorinated PCBs inhibit the human xenobiotic response mediated by the steroid and xenobiotic receptor (SXR). *Environ Health Perspect* **112:**163–169.

Watkins RE, Davis-Searles PR, Lambert MH, and Redinbo MR (2003) Coactivator binding promotes the specific interaction between ligand and the pregnane X receptor. *J Mol Biol* **331:**815–828.

Watkins RE, Wisely GB, Moore LB, Collins JL, Lambert MH, Williams SP, Willson TM, Kliewer SA, and Redinbo MR (2001) The human nuclear xenobiotic receptor PXR: structural determinants of directed promiscuity. *Science* **292:**2329–2333.

Wentworth JM, Agostini M, Love J, Schwabe JW, and Chatterjee VK (2000) St John's wort, a herbal antidepressant, activates the steroid X receptor. *J Endocrinol* **166:**R11–R16.

Xie W, Barwick JL, Simon CM, Pierce AM, Safe S, Blumberg B, Guzelian PS, and Evans RM (2000) Reciprocal activation of xenobiotic response genes by nuclear receptors SXR/PXR and CAR. *Genes Dev* **14:**3014–3023.

Xie W, Yeuh MF, Radominska-Pandya A, Saini SP, Negishi Y, Bottroff BS, Cabrera GY, Tukey RH, and Evans RM (2003) Control of steroid, heme, and carcinogen metabolism by nuclear pregnane X receptor and constitutive androstane receptor. *Proc Natl Acad Sci U S A* **100:**4150–4155.

Xue Y, Chao E, Zuercher WJ, Willson TM, Collins JL, Redinbo MR (2007a). Crystal structure of the PXR-T1317 complex provides a scaffold to examine the potential for receptor antagonism. *Bioorg Med Chem* **15:**2156–2166.

Xue Y, Moore LB, Orans J, Peng L, Bencharit S, Kliewer SA, Redinbo MR (2007b). Crystal structure of the PXR-estradiol complex provides insights into endobiotic recognition. *Mol Endocrinol* **21:**1028–1038.

Zhou C, Poulton EJ, Grun F, Bammler TK, Blumberg B, Thummel KE, Eaton DL (2007) The dietary isothiocyanate, sulforaphane is an antagonist of the human steroid and xenobiotic receptor (SXR). *Mol Pharmacol* **71:**220–229.

Zhou J, Zhai Y, Mu Y, Gong H, Uppal H, Toma D, Ren S, Evans RM, and Xie W (2006) A novel pregnane X receptor-mediated and sterol regulatory element-binding protein-independent lipogenic pathway. *J Biol Chem* **281:**15013–15020.

Address correspondence to: Patrick Balaguer, Equipe INSERM U824, Signalisation Hormonale, Environnement et Cancer, Centre de Recherche en Cancérologie de Montpellier (CRCM), Parc Euromédecine – CRLC Val d'Aurelle, F-34298 Montpellier, France Cedex 5. E-mail: p.balaguer@valdorel.fnclcc.fr